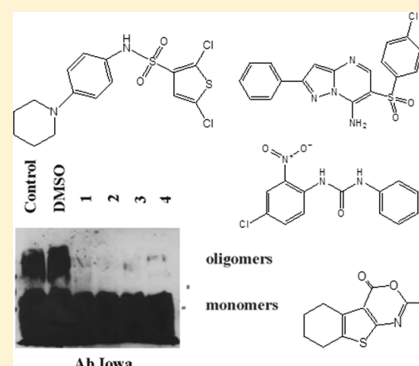


Discovery of Novel Inhibitors of Amyloid β -Peptide 1–42 AggregationLaura C. López,^{†,‡} Suzana Dos-Reis,^{§,||} Alba Espargaró,[⊥] José A. Carrodegua,^{†,‡} Marie-Lise Maddelein,^{§,||} Salvador Ventura,[⊥] and Javier Sancho^{*,†,‡}[†]Departamento de Bioquímica y Biología Molecular y Celular, Facultad de Ciencias, Universidad de Zaragoza, Pedro Cerbuna 12, 50009 Zaragoza, Spain[‡]Joint Unit BIFI-IQFR, CSIC, Biocomputation and Complex Systems Physics Institute (BIFI), Universidad de Zaragoza, Mariano Esquillor, Edificio I + D, 50018 Zaragoza, Spain[§]CNRS, IPBS (Institut de Pharmacologie et de Biologie Structurale), 205 route de Narbonne BP64182, F-31077 Toulouse, France^{||}UPS, IPBS, Université de Toulouse, F-31077 Toulouse, France[⊥]Institut de Biotecnologia i Biomedicina and Departament de Bioquímica i Biologia Molecular, Universitat Autònoma de Barcelona, Bellaterra, Barcelona, Spain

S Supporting Information

ABSTRACT: Alzheimer's disease, characterized by deposits of amyloid β -peptide ($A\beta$), is the most common neurodegenerative disease, but it still lacks a specific treatment. We have discovered five chemically unrelated inhibitors of the in vitro aggregation of the $A\beta$ 17–40 peptide by screening two commercial chemical libraries. Four of them (1–4) exhibit relatively low MCCs toward HeLa cells (17–184 μ M). The usefulness of compounds 1–4 to inhibit the in vivo aggregation of $A\beta$ 1–42 has been demonstrated using two fungi models, *Saccharomyces cerevisiae* and *Podospira anserina*, previously transformed to express $A\beta$ 1–42. Estimated IC_{50} s are around 1–2 μ M. Interestingly, addition of any of the four compounds to sonicated preformed *P. anserina* aggregates completely inhibited the appearance of SDS-resistant oligomers. This combination of HTP in vitro screening with validation in fungi models provides an efficient way to identify novel inhibitory compounds of $A\beta$ 1–42 aggregation for subsequent testing in animal models.



INTRODUCTION

Alzheimer's disease (AD)^{1–3} is the most common neurodegenerative disease causing dementia in humans. It affects around 30 million people worldwide, with an incidence of 10% in individuals older than 65⁴ and 30–40% in those beyond 85.^{5,6} Histologically, AD is characterized by the presence of extracellular senile plaques, mainly composed of amyloid β peptide ($A\beta$), and intracellular neurofibrillary tangles formed by hyperphosphorylated tau protein. The extracellular senile plaques are made of $A\beta$, mainly 40–42-residue long peptide fragments of the β -amyloid precursor protein (APP),⁷ which is encoded on chromosome 21.⁸ Down's syndrome individuals usually present $A\beta$ deposition at 30 years of age. The temporal profile of their $A\beta$ lesions indicates that the earliest deposits are diffuse or "preamyloid" plaques⁹ suggested to be mainly composed of $A\beta$ 17–42.¹⁰ Several $A\beta$ fragments are produced upon processing of APP, the 42-amino acid fragment ($A\beta$ 1–42) having the strongest aggregation capacity and being the predominant species in amyloid plaques.¹¹ Environmental factors have been also linked to formation of amyloid plaques.¹²

Although the in vitro and in vivo toxicities of $A\beta$ peptides and derived fragments have been demonstrated by several studies,¹³ identification of the major toxic species has remained

elusive. Recent findings have reported a direct relationship between early states of $A\beta$ aggregation and the severity of neuronal function impairment. Because those early aggregates are soluble, they have been termed $A\beta$ -derived diffusible ligands.¹⁴ So far there is no definitive treatment for AD. Approaches for therapeutic intervention in AD have focused on major steps of the $A\beta$ cascade: $A\beta$ production by proteolysis from APP, $A\beta$ aggregation, and inflammation caused by $A\beta$ deposition.¹⁵ Because neurotoxicity is mainly associated with the formation of $A\beta$ aggregates, inhibiting the process of $A\beta$ self-assembly has prompted the development of anti- $A\beta$ antibodies¹⁶ and the identification of β -sheet-disrupting compounds.¹⁷ In this respect, several antiaggregation compounds have been identified that can prevent neurotoxicity in vitro, but their use in vivo is often compromised by their toxicity, lack of specificity, inability to cross the blood–brain barrier, and/or unknown mechanism of action.^{18,19} Therefore, substantial therapeutic intervention is long overdue.

Target-oriented screening of large collections of chemically diverse compounds is a useful approach toward the discovery of

Received: May 31, 2012

Published: September 25, 2012

novel bioactive compounds exhibiting a specific effect on the target. For protein targets, common approaches include screening for inhibitors or for pharmacological chaperones.^{20,21} We report here the discovery of novel inhibitors of the aggregation of the A β 1–42 peptide. A two-step process has been used consisting of an initial high throughput, fluorescence-based aggregation assay of two large commercial libraries, followed by discrimination of false positives and confirmation of true positives by means of turbidimetry and electron-microscopy assays, respectively. Five structurally unrelated inhibitory compounds have been identified out of 11 250 assayed, which have been tested for in vivo activity against A β 1–42 aggregation using recently developed *Podospora*²² and yeast²³ models. Four of them are effective and appear to block the elongation of preformed aggregates.

RESULTS AND DISCUSSION

High Throughput Screening of Chemical Libraries Based on the Enhancement of Th T Fluorescence upon Binding to Aggregated A β . To detect aggregation of A β 17–40, a HTS method was devised based on the reported increase in fluorescence experienced by ThT upon binding to amyloid fibrils.²⁴ To speed the screening, a first round of aggregation kinetics was recorded with five different chemicals added per well. The compounds present in wells where inhibition of aggregation was observed were then tested individually under otherwise identical solution conditions in order to identify the actual positive compound.

The kinetics of amyloid fibril formation usually follows a sigmoidal curve that reflects a nucleation-dependent growth mechanism. The aggregation of A β 17–40 follows this kinetic scheme (Figure 1). The detected lag phase typically takes

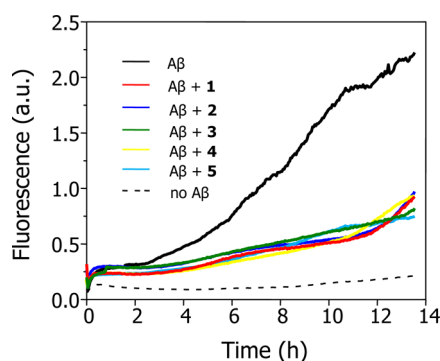


Figure 1. Inhibition of amyloid formation by five compounds monitored by ThT fluorescence. The ability of five different compounds to inhibit amyloid formation by A β 17–40 was determined following ThT fluorescence increase (excitation at 450 nm and emission at 500 nm) in a FluoDia T 70 fluorometer (Photal). Kinetics of aggregation were carried out in PBS buffer, at 37 °C for samples containing 6.5 μ M ThT (negative control), 6.5 μ M ThT plus 50 μ M A β 17–40 (positive control), or 6.5 μ M ThT plus 50 μ M A β 17–40 and 100 μ M compound.

around 3 h and is attributed to the formation of the initial nuclei on which the polymerization or fibril growth spontaneously proceeds with a concomitant increase in fluorescence in the presence of ThT. Figure 1 shows the effects exerted on the aggregation kinetics by the five compounds that were selected as true positive hits at the end of the screening. Apparently, these compounds slowed the nucleation step to up to 11 h. Therefore, the increase in

fluorescence observed in the kinetics when those compounds were present in the aggregating solution was clearly lower, and their effect was easily detected.

Turbidity Tests To Select True Positives. Identification of positive compounds by an assay based on detecting a reduction in the fluorescence intensity increase associated with aggregation is prone to producing many false positives because of fluorescence quenching due to absorbance from colored compounds. In addition to the five true positives found, thirty other compounds gave rise to apparent decreases in ThT fluorescence over the incubation period of 13 h, compared to the control. Although the potential quenching of ThT fluorescence by colored compounds could have been anticipated from a study of their spectroscopic properties, such an approach would have been slow and therefore inappropriate for an HTS method. More importantly, spectroscopic interference is not an indication of lack of an antiaggregative effect. Thus, we used a straightforward turbidimetry method to directly test whether the compounds initially identified in the fluorescence assay were true inhibitors of aggregation. A β aggregation gives rise to solution turbidity, which can be detected by monitoring absorbance at 360 nm. Therefore, 50 μ M A β 17–40 solutions were incubated for 10 h in the presence of tentative positives, and the absorbance at 360 nm was measured every 30 min. Because the aggregation profiles were not very reproducible, each compound tested was compared to a positive aggregation control run simultaneously and containing an aliquot of the same peptide solution. The kinetics of turbidity increase are shown in Figure 2. On the basis of them, only five compounds were selected as inhibitors of A β 17–40 aggregation among the 35 tentative positives identified in the previous fluorescence-based HTS step.

Transmission Electron Microscopy Analysis of the Effect of Inhibitors on Fiber Formation. The previous two-step selection strongly suggested that the five selected compounds exhibited an inhibitory effect on the aggregation of the A β 17–40 peptide. To further prove that A β 17–40 aggregation was inhibited by those compounds, we analyzed by transmission electron microscopy the occurrence and morphology of A β fibers grown in the absence and presence of the five selected compounds. Figure 3 shows that the five laterally associated or twisted fibrillar assemblies could only be observed in the untreated control containing A β , whereas in presence of inhibitor, small and rather amorphous aggregates appeared after 24 h incubation at 37 °C.

Chemical Nature and Cellular Toxicity of the Five Inhibitors. The chemical structures of the five inhibitors are shown in Figure 4. Compounds 1–4 are heterocycles showing no obvious chemical relationship apart from their similar molecular weights and log *P*: 221.3 and 2.8, 391.3 and 3.9, 291.7 and 3.7, and 384.8 and 3.3 for compounds 1, 2, 3 and 4, respectively. Neither of them contains asymmetric centers and variants can in principle be easily synthesized. They were present in the Maybridge collection, which includes thousands of compounds selected for their chemical diversity and drug likeness, most obeying Lipinsky's rules of 5.²⁵ Compound 5 is alexidine dihydrochloride, a commercial drug used as a disinfectant. This compound was present in the Hitfinder collection, which comprises marketed drugs.

To evaluate toxicity of the five inhibitors, we treated HeLa cells with different inhibitor concentrations ranging from 10 nM to 200 μ M. Toxicity was evaluated using the Cell Proliferation Kit II (Roche), which detects dehydrogenase

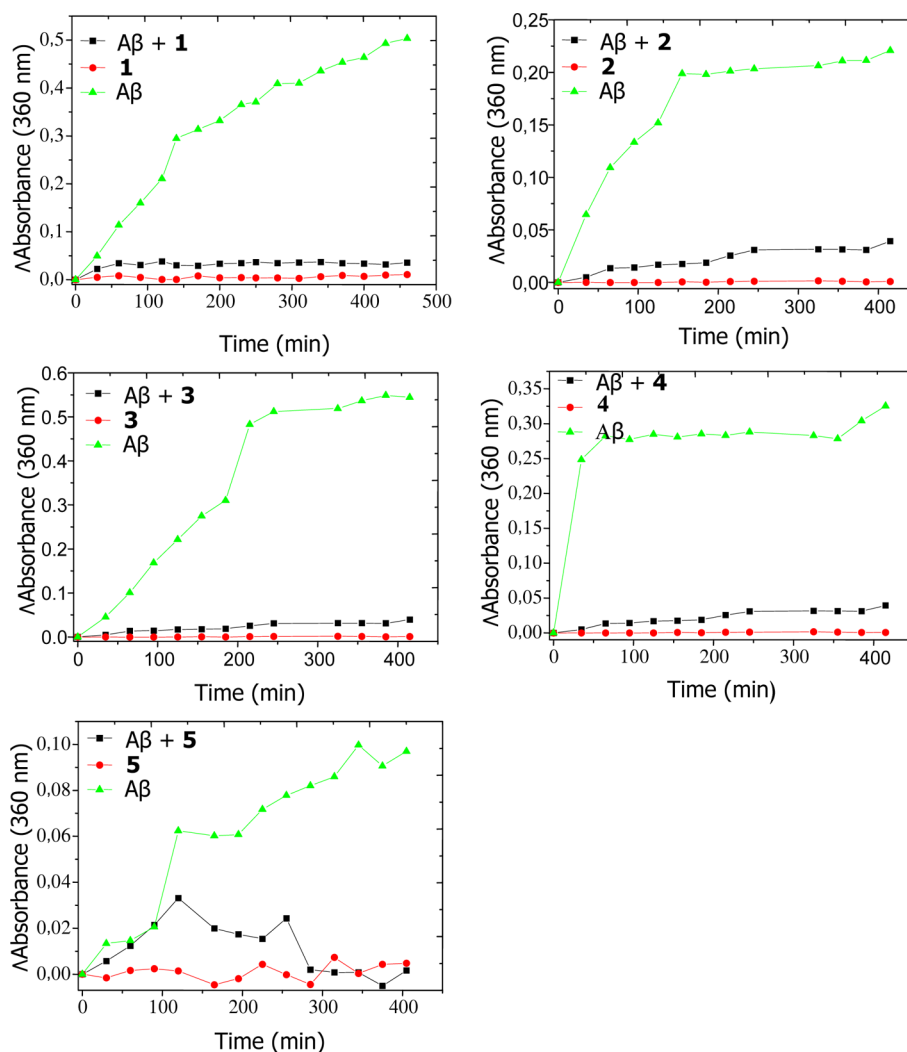


Figure 2. Inhibition of amyloid formation by five compounds, monitored by turbidity. Turbidity kinetic assays of A β 17–40 aggregation alone (green triangles) or in the presence of 50 μ M of different inhibitory compounds (black squares) are shown together with negative controls (buffer solution with no peptide) in red circles.

activity by reduction of a tetrazolium salt, XTT, to a soluble formazan. The toxicity curves used to calculate minimal cytotoxic concentrations are shown in Figure 5. The most toxic compound was alexidine, (MCC = 2 μ M) while the less toxic one was compound 1 (MCC = 184 μ M). Compounds 2, 3 and 4 displayed intermediate MCCs of 17, 20, and 22 μ M, respectively. On the basis of these data and of toxicity tests performed in yeast and in *Podospora* (see below), the potential inhibitory effect of compound 5 was not further tested.

In Vivo Testing of Compounds 1–4 in Yeast Cells Expressing A β 1–42 Fused to h-DHFR. We have recently developed an assay in which the intracellular aggregation of proteins correlates with cell viability in yeast.²³ The assay is based on the fusion of the target protein to the human dihydrofolate reductase (h-DHFR) gene, whose intracellular activity acts as a reporter of the aggregational state of the fusion protein in yeast in the presence of the h-DHFR inhibitor methotrexate (MTX). In this system, aggregation-prone proteins render cells MTX sensitive. The assay has been successfully applied to study the intracellular aggregation of A β 1–42, α -synuclein, and polyQ repeats.²³ In addition, using the yeast strain *erg6D* that contains a mutation enhancing membrane fluidity and permeability to chemical compounds,

the assay allows identifying molecules able to modulate the early stages of aggregation in living cells. Here, we monitored the ability of 1–4 to prevent the aggregation of an A β 1–42-h-DHFR fusion inside *erg6D* cells by measuring their impact on viability in the presence of 10 or 20 μ M MTX. The inhibitors were added to the cell medium at 10 and 100 μ M final concentrations. However, compounds 3 and 4 displayed significant toxicity at 100 μ M and were only assayed at 10 μ M, while compound 5 was toxic for yeast cells already at 10 μ M and was not tested. As a trend, the antiaggregational effect of the compounds was more evident in the presence of 20 μ M MTX, where cell physiology is more compromised. Compounds 1, 2, and 3 significantly increased the viability of cells expressing A β 42-h-DHFR at 10 μ M, relative to control cells grown in the absence of compounds (Figure 6). For compounds 1 and 2, each tested at two different concentrations, the effect was dose-dependent. In particular, the cell survival effect promoted by compound 2 was comparable to that exerted by validated A β 1–42 aggregation inhibitors such as quercetin or apigenin. Rough estimates of IC₅₀ values can be derived for compounds 1–4 by previously comparing the effect of reference inhibitors in the yeast growth restoration assay with their reported IC₅₀s. Table S1 (Supporting Information)

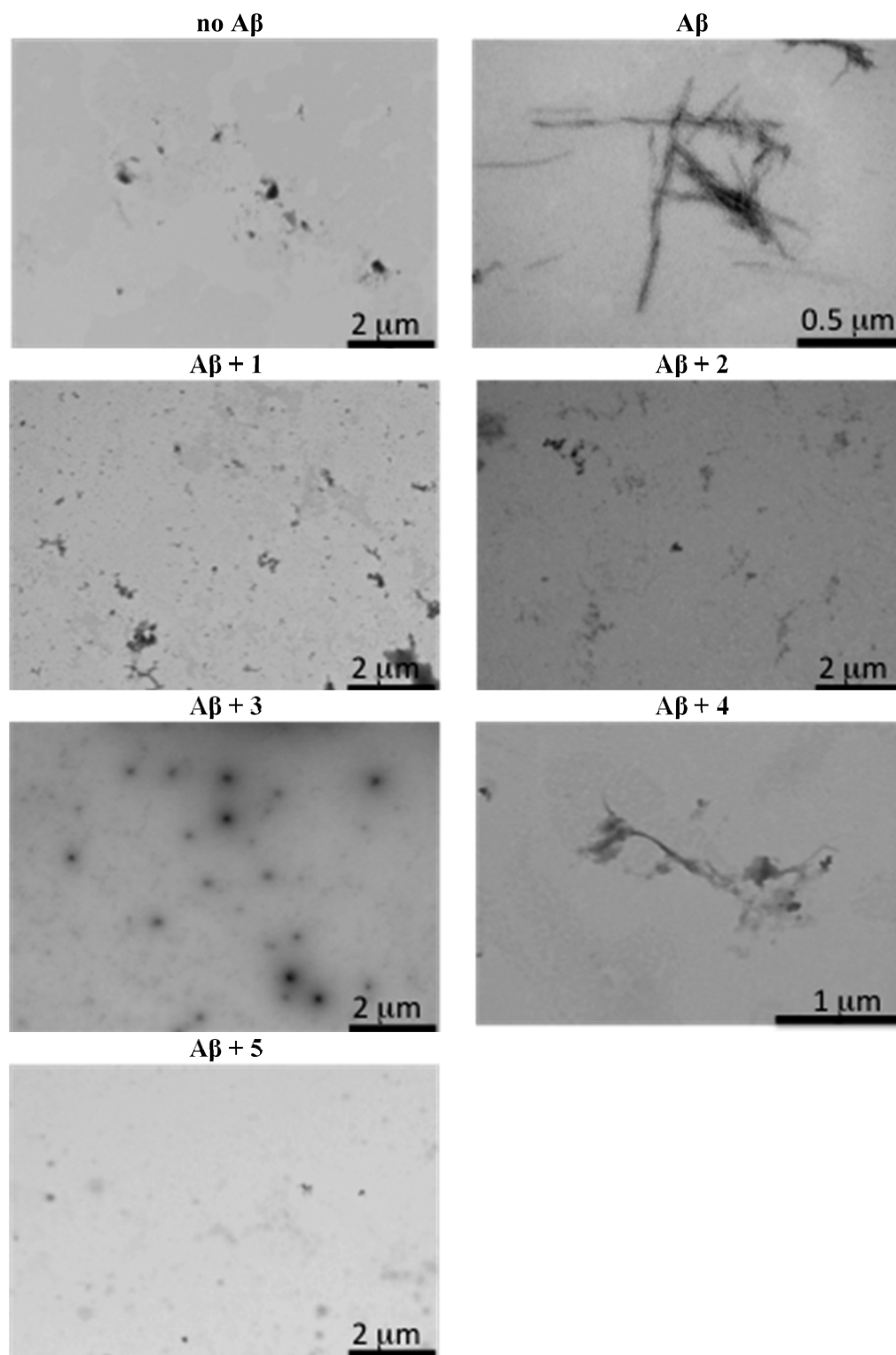


Figure 3. Inhibition of amyloid formation by five compounds, monitored by transmission electron microscopy. Negatively stained electron microscopy performed on a sample of $A\beta_{17-40}$ ($50 \mu\text{M}$) in the absence (negative control) or individual presence of five compounds ($100 \mu\text{M}$ each) after incubation at 37°C for 24 h.

summarizes the IC_{50} oligomerization for seven aggregation inhibitors together with their effect in the yeast growth restoration assay performed as here described for compounds 1–4. Figure S1A (Supporting Information) shows there is a correlation between the growth restoration efficacy and the log IC_{50} ($r = 0.71$), which increases to $r = 0.86$ (Figure S1B) if one

outlier (Thioflavin T) is left aside. From these two correlations, the IC_{50} for compounds 1–4 can be estimated to be between around 2.1–1.2, 1.2–0.7, 1.6–0.9, and 4.6–2.3 μM , respectively.

Mechanistic Insight into the Inhibitory Action of Compounds 1–4 by in Vivo Testing in *Podospora* Cells

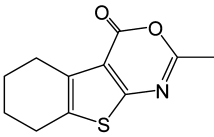
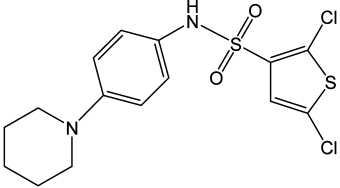
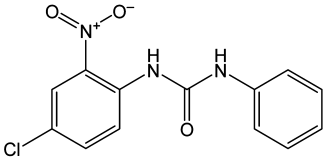
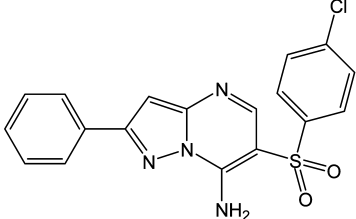
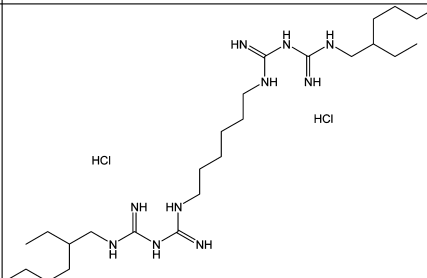
<p>Compound 1</p> <p>2-methyl-5,6,7,8-tetrahydro-4H-[1]benzothieno[2,3-d][1,3]oxazin-4-one</p>	
<p>Compound 2</p> <p>2,5-dichloro-N-(4-piperidinophenyl)-3-thiophenesulfonamide</p>	
<p>Compound 3</p> <p>N-(4-chloro-2-nitrophenyl)-N'-phenylurea</p>	
<p>Compound 4</p> <p>6-[(4-chlorophenyl)sulfonyl]-2-phenylpyrazolo[1,5-a]pyrimidin-7-amine</p>	
<p>Compound 5</p> <p><i>Alexidine dihydrochloride</i> <i>N,N'</i>-Bis(2-ethylhexyl)-3,12-diimino-2,4,11,13-tetraazatetradecanediiimidamide dihydrochloride</p>	

Figure 4. Names and chemical structures of five inhibitors of $A\beta$ aggregation. These five compounds inhibit the aggregation of $A\beta_{17-40}$ in vitro. Additionally, compounds 1–4 inhibit the in vivo aggregation of $A\beta_{1-42}$ in two fungi models: *Podospora anserina* and *Saccharomyces cerevisiae* (see Discussion).

Expressing $A\beta_{1-42}$. *Podospora anserina* is a filamentous fungus that has been shown to be a valuable model to study amyloid aggregation and toxicity.^{22,26–28} To characterize $A\beta$ aggregation in this model organism, several vectors have been constructed expressing either $A\beta_{1-42}$ alone or fused to the green fluorescence protein (GFP). For fluorescence analysis, insertion of a linker between GFP and $A\beta$ was necessary to allow the GFP to fold correctly. The HeLo domain of the protein HET-s was chosen because of its flexibility, allowing folding modification of the adjacent C-terminus domain.²⁸ Before evaluating the effect of the four compounds on $A\beta$ aggregation in *Podospora anserina*, we first observed whether they modified the fluorescence distribution of GFP- $A\beta_{1-42}$ expressing strains (Figure S2, Supporting Information). Confocal microscopy observation of the transformants grown in presence of any of the compounds showed a global reduction of fluorescence intensity, which for compounds 3 and 5 was

associated with an intense vacuolization. Fluorescence foci from strains grown in control media were no longer present in strains grown on media containing 2, 3, or 4. Compound 5 was not further tested because of its severe toxicity toward *Podospora*. The toxicity of the compounds was probed via their impact on *Podospora* lifespan. For this study, senescence tests were performed on 12 transformants expressing either the vector alone or $A\beta_{1-42}$ or $A\beta_{1-42}$ Iowa ($A\beta_{1-42}$ carrying Iowa familial mutation). Compared to DMSO 10% alone, 1 at 100 μM and 3 at 50 μM reduced the lifespan and the growth rate of the fungi (Figure S3 and Table S2, Supporting Information). However, neither 50 μM 2 nor 50 μM 4 affected the growth rate and the average lifespan of the transformants expressing GFP- $A\beta_{1-42}$, which was similar to the control.

Biochemical analysis of *Podospora* crude extracts indicated that $A\beta$ expression from all the constructs led to accumulation of SDS resistant oligomers (not shown). To characterize the

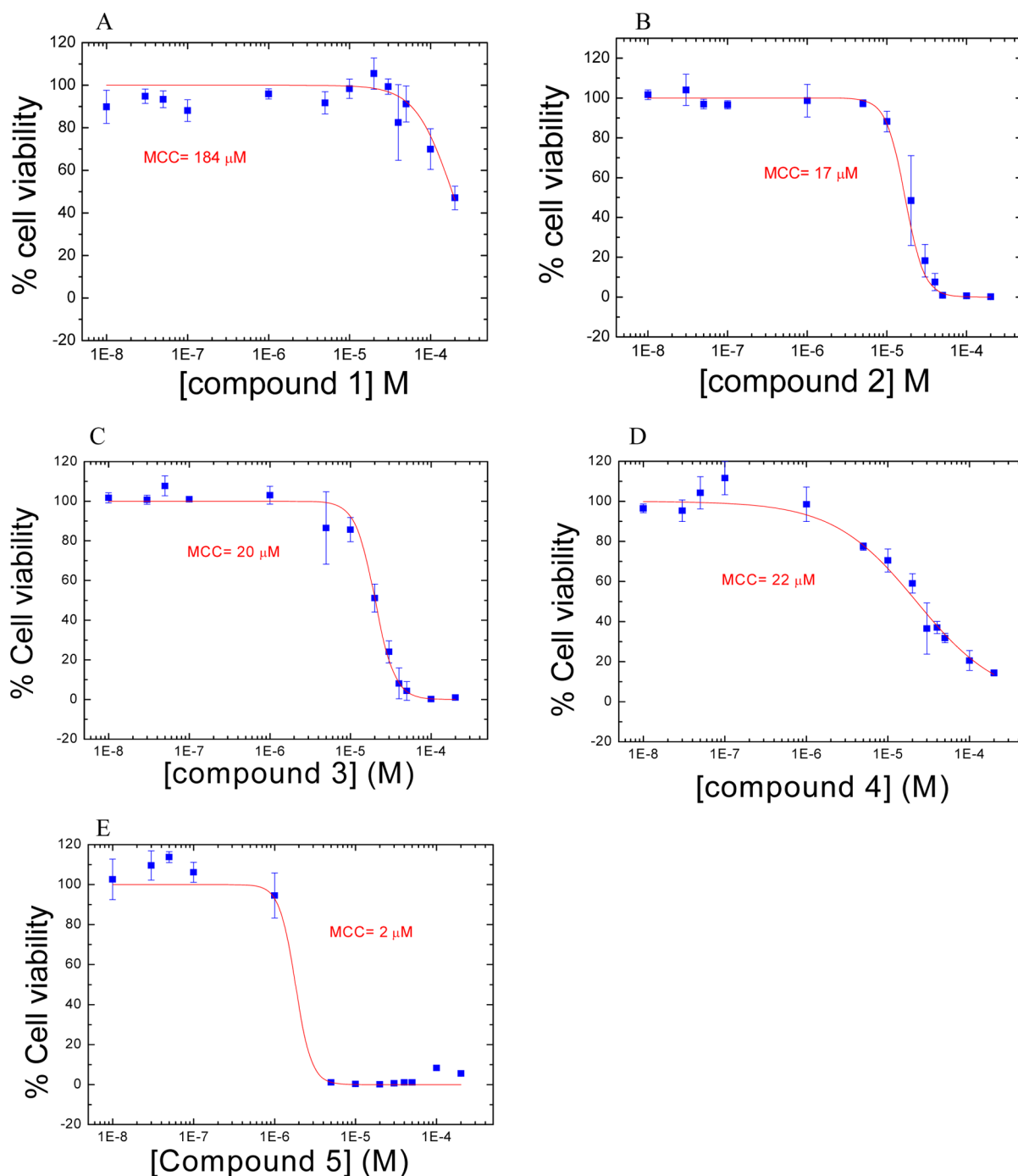


Figure 5. Minimal cytotoxic concentrations (MCC) of five inhibitors of $A\beta_{17-40}$ aggregation. HeLa cells (30 000 cells/100 μ L) were grown for 24 h and then treated with different concentrations of each of the five inhibitors. Cell viability was determined by measuring XTT reduction. Means \pm SE are shown for different inhibitor concentrations. MCC are the concentrations of inhibitor allowing for 50% viability according to the fit of the experimental data.

effect of the compounds on $A\beta$ aggregation we used transformants expressing GFP- $A\beta_{1-42}$ Iowa, accumulating large amounts of oligomers. Thus, after cultivation in complete media for four days, 10% DMSO and either 100 μ M of **1** or 50 μ M of **2**, **3**, or **4** were added 24 h before collecting the crude extracts. $A\beta$ SDS-resistant oligomers were revealed by 8% SDS-PAGE and Western-Blot analysis. As shown in Figure 7a, presence of the compound **2** but not **1**, **3**, or **4** in the culture media reduced the amount of large SDS-resistant oligomers compared to the DMSO control. Interestingly, compound **2**

was also the most effective one in the growth restoration assays in yeast (Figure 6).

A time course assay of the effect of compounds on $A\beta$ aggregation in *Podospora* was carried out on a strain expressing GFP- $A\beta_{1-42}$, which forms less aggregates than that of $A\beta_{1-42}$ Iowa. The different compounds were added to the growth media from 10 h to 5 days prior to collecting the mycelia. In all cases, the compounds reduced the amount of SDS-resistant oligomers of higher molecular weight. The effect of compounds **2** and **3** (Figure 7b) can be observed as soon as after 10 h of

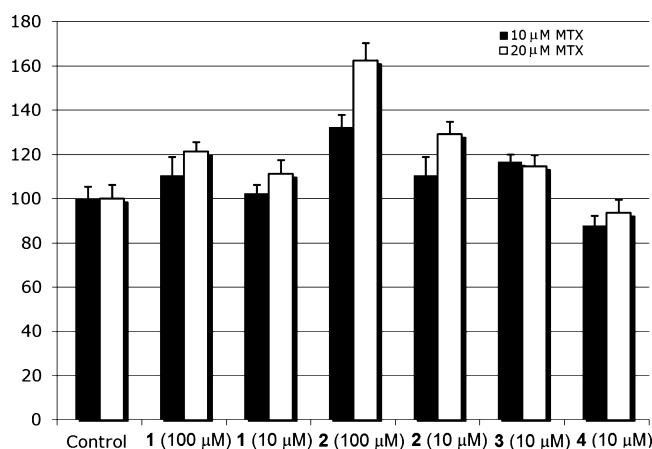


Figure 6. Effect of compounds on $A\beta$ 1–42 aggregation in yeast. Growth restoration of *erg6D* yeast cells expressing $A\beta$ 1–42–DHFR in the presence of 10 or 20 μ M MTX, and selected concentrations of the tested compounds. Growth is normalized to 0 μ M compound and the growth of cells expressing DHFR alone.

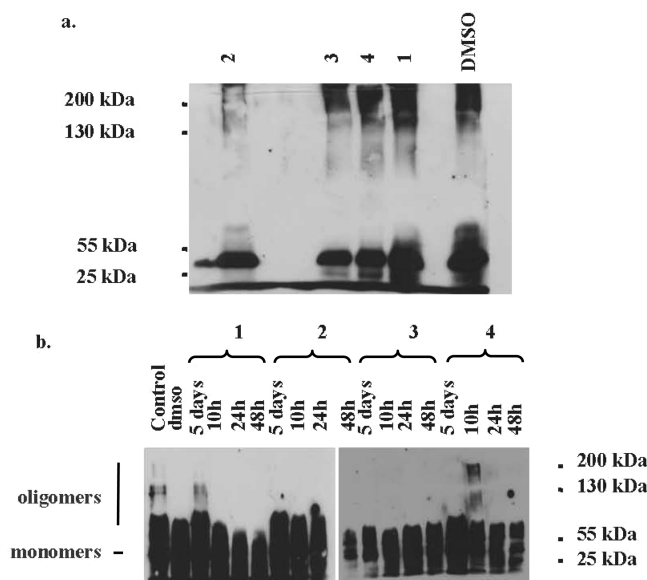


Figure 7. Biochemical analysis of the effect of compounds on 2% SDS resistant $A\beta$ 1–42 aggregates in *Podospora*. Crude extracts of *Podospora* strains expressing GFP– $A\beta$ 1–42 Iowa (a) or GFP– $A\beta$ 1–42 (b) analyzed by 8% SDS-PAGE and Western blot after cultivation in complete media containing 10% DMSO and either 100 μ M of 1 or 50 μ M of 2, 3, or 4 for 24 h (a), and for 10 h, 24 h, 48 h, or 5 days (b). GFP– $A\beta$ 1–42 monomers migrated at around 45 kDa. Blots were probed with anti $A\beta$ antibody NAB228.

treatment and persists after 5 days. Compound 1 is also efficient at 10 h of treatment but the effect fades after 5 days (Figure 7b). Compound 4 reduced aggregate formation after 24 h, and the effect was persistent. On the basis of their early effect and persistence, compounds 2 and 3 seems to be, compared to compounds 1 and 4, the more effective ones in avoiding the accumulation of SDS-resistant aggregates in *Podospora* expressing GFP– $A\beta$ 1–42, in agreement with their more positive effects in the growth restoration assays in yeast (Figure 6).

The low content of high molecular weight aggregates in cells treated with compounds 1–4 may be due to inhibition of aggregate growth, as demonstrated in the *in vitro* assays

(Figures 1–3), but it could also be due to the compounds being able to dissolve preformed aggregates. To test whether compounds 1–4 could dissolve preformed aggregates, crude extracts containing $A\beta$ aggregates were mixed with each of the compounds and incubated 1 h at 4 $^{\circ}$ C, before semidenaturing detergent agarose gel electrophoresis (SDD-AGE) analysis. Only compound 3 slightly reduced the amount of SDS resistant $A\beta$ oligomers, and only for wild type $A\beta$ 1–42 expressing strains (Figure S4). This indicates that the compounds do not significantly dissolve preformed aggregates. To confirm that the compounds may, in fact, affect oligomers assembly, as suggested by the *in vitro* tests (Figures 1–3), we sonicated crude extracts previously mixed with each of the four compounds. After sonication, the extracts were incubated for 1 h at 4 $^{\circ}$ C. WB analysis of SDS resistant oligomers showed small size oligomers (Figure 8, right panel) of around 100–130

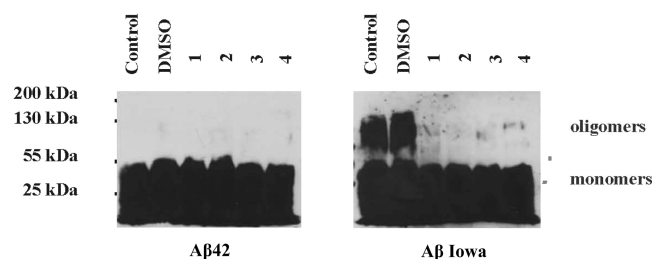


Figure 8. Effect of the compounds on the elongation of $A\beta$ 1–42 aggregates contained in crude extract of *Podospora* and previously sonicated. 8% SDS PAGE of crude extracts of strains expressing GFP– $A\beta$ 1–42 (left panels) or GFP– $A\beta$ 1–42 Iowa (right panels) revealed with anti- $A\beta$ antibody NAB228. The extracts were incubated for 1 h after sonication before they were loaded on the gel.

kDa (tentatively attributed to trimers of the GFP– $A\beta$ 1–42) from $A\beta$ 1–42 Iowa-containing extracts sonicated and incubated in buffer alone or in 10% DMSO. Clearly, those trimers were missing from $A\beta$ 1–42 Iowa-containing crude extracts treated with either one of the compounds. They were also absent from the sonicated extracts of the GFP– $A\beta$ 1–42 expressing strain (Figure 8, left panel). Comparison of the sonicated extracts in the presence and absence of compounds 1–4 of the more aggregation-prone Iowa peptide confirms that these four compounds interfere with oligomer growth at early stages of aggregation. It is possible that they interact with and impede the elongation of the dimers.

CONCLUSIONS

Five chemically unrelated compounds that interfere with $A\beta$ 17–40 aggregation *in vitro* have been identified. Among them, the four compounds exhibiting lower toxicity have been further tested in two fungi model organisms, *Podospora anserina* and *Saccharomyces cerevisiae*, expressing $A\beta$ 1–42 fused to reporter proteins. Those four compounds appear to interfere with early stages of $A\beta$ 1–42 oligomerization, and at least two of them, compounds 2 and 3, significantly reduced the intracellular aggregation of the expressed $A\beta$ 1–42 fusions upon addition to the culture medium of the fungi model organisms. The structural modifications induced by these compounds on $A\beta$ 1–42 aggregates will be the subject of further investigations.

EXPERIMENTAL SECTION

Chemicals, Amyloid β Peptide ($A\beta$ 17–40), and Chemical Libraries. Thioflavin T (ThT) and amyloid β peptide ($A\beta$ 17–40;

more than 98% pure by HPLC) were purchased from American Peptide Company, Inc. (Sunnyvale, CA). A 500 μM peptide stock solution was prepared by dissolving lyophilized peptide in 0.02% NH_4OH . To remove aggregates, the solution was centrifuged at 14 000 rpm for 30 min at 4 $^\circ\text{C}$ before use, and the actual peptide concentration was determined from the ratio of absorbances at 214 nm of the stock and filtered solutions. Methotrexate (MTX) and sulfanilamide were purchased from Sigma Aldrich.

Chemical libraries were purchased from Maybridge (Hit Finder Collection, 10 000 compounds) and from Prestwick Chemicals (The Prestwick Chemical Library, 1120 compounds). The Hitfinder collection contains chemically diverse compounds, most of which follow Lipinski's rules,²⁵ while the Prestwick collection contains only marketed drugs. The chemicals in either library have purities greater than 90%, as determined by LCMS.

High Throughput Thioflavin T Binding Assay. Thioflavin T is a fluorophore that experiences a large increase in fluorescence upon binding to amyloid fibrils. ThT was prepared as a 650 μM stock solution in 10 mM NaH_2PO_4 , 150 mM NaCl , pH 7.0 (PBS buffer).

The initial screening of the two libraries was carried out using 96-well plates, each well containing, in 200 μL of PBS, 50 μM $\text{A}\beta$ 17–40, 6.5 μM ThT, and five different compounds at 100 μM each. ThT fluorescence was measured using a FluoDia T 70 fluorometer (Photal) with excitation and emission wavelengths of 450 and 500 nm, respectively. Aggregation kinetics were carried out at 37 $^\circ\text{C}$ for 13 h. Measurements were made every 153 s, with a 3-s shaking step before each measurement.

Turbidimetry Assay. To identify false positives, 50 μM $\text{A}\beta$ 17–40 was mixed with 100 μM compound in PBS buffer in a quartz cuvette (Hellma 104QS with 10 mm light path), and aggregation kinetics were followed by recording the absorbance at 360 nm, every 30 min, over 10 h, in a Varian Cary 100 Bio spectrophotometer.

Transmission Electron Microscopy. Transmission electron microscopy analysis was performed to observe size and structural morphology changes of $\text{A}\beta$ 17–40 fibrils in presence and absence of selected compounds. The samples were examined under a Hitachi H-7000 transmission electron microscope at 75 kV. Fresh samples were prepared mixing 20 μL of $\text{A}\beta$ 17–40 stock solution (500 μM $\text{A}\beta$ in 0.02% NH_4OH) with 20 μL of compound stock solution (1 mM compound in 10% dimethyl sulfoxide: DMSO) plus 160 μM of PBS buffer. The samples were incubated at 37 $^\circ\text{C}$ for 24 h. Then, a 5 μL -drop of each sample was placed on Formvar carbon support film on a copper grid (400 mesh) and stained with a 2% uranyl acetate solution in deionized Milli-Q water for 1 min. Excess stain was removed, and samples were dried at room temperature.

Cytotoxicity Assay. Cytotoxicity of five selected chemical compounds was studied using HeLa cells cultured in Dulbecco's Modified Eagle Medium (DMEM) medium supplemented with 100 U/mL penicillin, 100 $\mu\text{g}/\text{mL}$ streptomycin sulfate, and 10% fetal calf serum (all reagents from Invitrogen) at 37 $^\circ\text{C}$ in a 5% CO_2 atmosphere. Cells were cultured in 25 mL polystyrene tissue culture flasks and subcultured every 3 days. To test the toxicity of compounds, HeLa cells were aliquoted in 96-well plates (3×10^4 cells per well in 100 μL of media). After incubation for 24 h in the absence or presence of each compound at different concentrations ranging from 10 nM to 200 μM , cell viability was assayed using 2,3-bis(2-methoxy-4-nitro-5-sulfophenyl)-5-[(phenylamino)carbonyl]-2H-tetrazolium hydroxide (XTT) (Cell Proliferation Kit II, Roche) following the manufacturer's instructions. Briefly, after the incubation period, cell media was replaced with 100 μL of DMEM, and 50 μL of XTT reagent was added to each well. The plates were incubated at 37 $^\circ\text{C}$ for 4 h in a humidified 5% CO_2 atmosphere. Optical density was read at 450 nm, with the reference filter set to 620 nm, using a spectrophotometric plate reader. The values obtained for controls lacking added compounds were considered to reflect 100% viability. Minimal cytotoxic concentrations (MCC) were calculated for each of the five tested compounds by fitting the viability at the different concentrations of compound to a dose–response function with variable Hill slope, as implemented in Origin Pro 8 (Northampton, MA) software.

Screening of Antiaggregational Compounds in Yeast. The yeast drug-permeable strain *erg6 Δ* in the BY4741 parental background (MAT a his3 Δ 0 leu2 Δ 0 met15 Δ 0 ura3 Δ 0) was used. Human dihydrofolate reductase (h-DHFR) as well as the fusion between $\text{A}\beta$ 1–42 and h-DHFR was expressed from a pESC(-Ura) plasmid. Yeast transformation was performed using the standard lithium/polyethylene glycol method. Cells were grown overnight at 30 $^\circ\text{C}$ in a selective synthetic medium containing raffinose. Pregrown yeast cells were diluted to an optical density of 0.02 at 600 nm in a minimal medium containing 1 mM of sulfanilamide and the appropriate concentration of each compound. This incubation step is performed to ensure the presence of the tested compound in the cell before protein expression. After 90 min, 2% galactose and 10 μM or 20 μM MTX were added to cultures. Cells were incubated at 30 $^\circ\text{C}$ for 20 h. The absorbance was measured using a Cary 400Bio spectrophotometer. The same experiment was performed with appropriate concentrations of DMSO as a control. In all the experiments OD₆₀₀ values reported are the averages of triplicate measurements. The toxicity of compounds was assessed in control cells expressing h-DHFR whereas their antiaggregation potency was tested in cells expressing the $\text{A}\beta$ 1–42-h-DHFR fusion.

Study of $\text{A}\beta$ Aggregation in *Podospora anserina*. $\text{A}\beta$ 1–42 expressing vector, called T10, was constructed by inserting the $\text{A}\beta$ 1–42 sequence in a pAN8.1 vector²⁹ using restriction sites NcoI/XmaI. The $\text{A}\beta$ 42 sequence was amplified by polymerase chain reaction (PCR) from the pCL12 template³⁰ (gift from C. D. Link) using the following primers: 5TC42OPT: 5'-CATGCCATGGACACTAGT-GATGCAGAATTCGGACATGACTCAGGATATGAA-3' and 3Xmab: 5'-TCCCGGGTCACGCTATGACAACACCGCCCATCAT-3', adding a SpeI restriction site in 5' of the $\text{A}\beta$ 1–42 sequence. The GFP sequence was amplified from the pBC1004 HET-s-GFP²⁶ by PCR using the following primers: 5GFNCO: 5'-CATGCCATGGT-GAGCAAGGGCGAGGAGCTGTTCCACCGGGGTGGTGCC-CATCCTGGTCGAGCTGGACGGCGACGTA-3' and 3GFxb: 5'-ATCACATGGTCTCTGCTGGAGTTTCGT-GACCCCGCCGGGATCACTCTCGGATGGACGAGCTGTACAAGTCTAGAGCA-3' to be cloned in the N-terminus of $\text{A}\beta$ 1–42 in the plasmid T10 restricted with NcoI and SpeI. The resulting vector, called T10GB4, expressing GFP– $\text{A}\beta$ 1–42 was mutagenized to introduce a HindIII site between GFP and the $\text{A}\beta$ 1–42 sequence using the following primers: 5GFHDab: 5'-CATGGACGAGCTGTACAAAAGCTTTACTAGTGATGCAGAATT-3' and 5GFHDab: 5'-AATTCTGCATCACTAGTAAAGCTTTTGTACAGCTCGTC-CATG-3' (Quick Change Site-Directed Mutagenesis Kit from Stratagene). The sequence coding for amino acids 3–225 corresponding to the HeLo domain of HET-s was amplified by PCR using the template pBC1004-Het-s-GFP and the following primers: 5SHDHETS: 5'-A A C C C A A G C T T T G C A G A A C C G T T C G G - G A T C G T T G C T G G C G C C T T G A A C G T T G C C G G C C T C T T - 3' and 3XBA225: 5'-TTGCTCTAGACCTTCCCACAATCGCGTC-GATCTTCTGCGCAGCCGCATCAGACATAGCTGCG-3', and cloned in T10GB4 digested with HindIII and XbaI.

The resulting vector, called RV52, expresses GFP–HeLo- $\text{A}\beta$ 42 under the GPD promoter. Familial Alzheimer mutation Iowa (D23N) was introduced by site-directed mutagenesis using the following primers: 5D23N: 5'-GTGTTCTTTGCAGAAAATGTGGGTT-CAAAC-3' and 3D23N: 5'-TGTTTGAACCCACATTTTCTG-CAAAGAACAC-3'. All the constructs were confirmed by DNA sequencing (Cogenics, Takeley, UK).

Media and growth conditions were as previously described (<http://podospora.igmors.u-psud.fr/>; accessed Aug 11, 2012). Senescence assays were performed on M2 solid media double agar on 150 \times 150 mm plates. The lifespan of a strain was evaluated by the replicative growth distance (cm) and time (day) from the explant to the senescence bar.³¹ For each condition, 12 transformants of the S strain expressing GFP– $\text{A}\beta$ were studied. Compounds were resuspended in 100% DMSO before being added to the media at a final concentration of 100 μM for 1 and 50 μM for 2 to 5, plus 10% DMSO in all cases. Fluorescence analysis was performed as described²⁷ using a Confocal Zeiss LSM 510 Axiovert microscope. For sodium dodecyl sulfate

(SDS) resistant aggregates analysis, the mycelia were collected after 5 days of growth and harvested in 100 mM Tris HCl, 50 mM NaCl, 0.5% Triton, pH 7.4. Cell debris was removed by low speed centrifugation, and crude extracts were incubated 10 min at 37 °C in a Laemmli buffer with 2% SDS before loading on 8% SDS PAGE or SDD-AGE.³² Blots were probed with anti A β antibody NAB228 (Sigma).

■ ASSOCIATED CONTENT

● Supporting Information

Additional information as noted in the text. This material is available free of charge via the Internet at <http://pubs.acs.org>

■ AUTHOR INFORMATION

Corresponding Author

*Tel: (+34) 976761286. E-mail: jsancho@unizar.es.

Notes

The authors declare the following competing financial interest(s): There are patents pending on compounds 1–4.

■ ACKNOWLEDGMENTS

L.C.L. is a recipient of a doctoral fellowship awarded by Consejo Superior de Investigaciones Científicas, JAE program. Studies performed by M.L.M. and S.D. were supported by the Fondation pour la Recherche Médicale (FRM), ATIP program of CNRS and UPS Toulouse 3 and the Community work of Pyrennes (CTP program with Midi-Pyrennes Region grant 09013560). S.V. acknowledges financial support from grants BFU2010-14901 from Ministerio de Ciencia e Innovación (Spain), 2009-SGR-760 and 2009-CTP-00004 from AGAUR (Generalitat de Catalunya). S.V. has been granted an ICREA Academia award (ICREA). J.S. acknowledges financial support from grants BFU2010-16297 [Ministerio de Ciencia e Innovación (Spain)] and PI078/08 and CTPR02/09 (DGA, Spain).

■ ABBREVIATIONS USED

A β , amyloid β peptide; AD, Alzheimer's disease; APP, β -amyloid precursor protein; DMEM, Dulbecco's Modified Eagle Medium; DMSO, dimethyl sulfoxide; GFP, green fluorescent protein; h-DHFR, human dihydrofolate reductase; HPLC, high-pressure liquid chromatography; HTS, high throughput screening; LCMS, liquid chromatography–mass spectrometry; MCC, minimal cytotoxic concentrations; MTX, methotrexate; PCR, polymerase chain reaction; SDS, sodium dodecyl sulfate; SDS-AGE, semidenaturing detergent agarose gel electrophoresis; ThT, Thioflavin T; XTT, 2,3-bis(2-methoxy-4-nitro-5-sulphophenyl)-5-[(phenylamino)carbonyl]-2H-tetrazolium hydroxide

■ REFERENCES

- (1) Alzheimer, A. Über eine eigenartige Erkrankung der Hirnrinde. *Allg. Z. Psychiatr. Psych.-Gerichtl. Med.* **1907**, *64*, 146–148.
- (2) Selkoe, D. J. Alzheimer's disease. *Cold Spring Harbor Perspect. Biol.* **2011**, *3*, a004457.
- (3) Holtzman, D. M.; Morris, J. C.; Goate, A. M. Alzheimer's disease: the challenge of the second century. *Sci. Transl. Med.* **2011**, *3*, 77sr1.
- (4) Hebert, L. E.; Scherr, P. A.; Bienias, J. L.; Bennett, D. A.; Evans, D. A. Alzheimer disease in the US population: prevalence estimates using the 2000 census. *Arch. Neurol.* **2003**, *60*, 1119–1122.
- (5) O'Brien, J. A.; Caro, J. J. Alzheimer's disease and other dementia in nursing homes: levels of management and cost. *Int. Psychogeriatr.* **2001**, *13*, 347–358.

(6) Stevens, T.; Livingston, G.; Kitchen, G.; Manela, M.; Walker, Z.; Katona, C. Islington study of dementia subtypes in the community. *Br. J. Psychiatry* **2002**, *180*, 270–276.

(7) Yamada, K.; Ren, X.; Nabeshima, T. Perspectives of pharmacotherapy in Alzheimer's disease. *Jpn. J. Pharmacol.* **1999**, *80*, 9–14.

(8) Selkoe, D. J. Normal and abnormal biology of the beta-amyloid precursor protein. *Annu. Rev. Neurosci.* **1994**, *17*, 489–517.

(9) Giaccone, G.; Tagliavini, F.; Linoli, G.; Bouras, C.; Frigerio, L.; Frangione, B.; Bugiani, O. Down patients: extracellular preamyloid deposits precede neuritic degeneration and senile plaques. *Neurosci. Lett.* **1989**, *97*, 232–238.

(10) Lalowski, M.; Golabek, A.; Lemere, C. A.; Selkoe, D. J.; Wisniewski, H. M.; Beavis, R. C.; Frangione, B.; Wisniewski, T. The "nonamyloidogenic" p3 fragment (amyloid beta 17–42) is a major constituent of Down's syndrome cerebellar preamyloid. *J. Biol. Chem.* **1996**, *271*, 33623–33631.

(11) Bitan, G.; Kirkitadze, M. D.; Lomakin, A.; Vollers, S. S.; Benedek, G. B.; Teplow, D. B. Amyloid beta-protein (A β) assembly: A β 40 and A β 42 oligomerize through distinct pathways. *Proc. Natl. Acad. Sci. U.S.A.* **2003**, *100*, 330–335.

(12) Kelly, J. W. The environmental dependency of protein folding best explains prion and amyloid diseases. *Proc. Natl. Acad. Sci. U.S.A.* **1998**, *95*, 930–932.

(13) Selkoe, D. J. Alzheimer's disease: genes, proteins, and therapy. *Physiol. Rev.* **2001**, *81*, 741–766.

(14) Walsh, D. M.; Selkoe, D. J. Oligomers on the brain: the emerging role of soluble protein aggregates in neurodegeneration. *Protein Pept. Lett.* **2004**, *11*, 213–228.

(15) Grundman, M.; Thal, L. J. Treatment of Alzheimer's disease: rationale and strategies. *Neurol. Clin.* **2000**, *18*, 807–828.

(16) Thatté, U. AN-1792 (Elan). *Curr. Opin. Invest. Drugs (BioMed Cent.)* **2001**, *2*, 663–667.

(17) Findeis, M. A.; Molineaux, S. M. Design and testing of inhibitors of fibril formation. *Methods Enzymol.* **1999**, *309*, 476–488.

(18) Re, F.; Airolidi, C.; Zona, C.; Masserini, M.; La Ferla, B.; Quattrocchi, N.; Nicotra, F. Beta amyloid aggregation inhibitors: small molecules as candidate drugs for therapy of Alzheimer's disease. *Curr. Med. Chem.* **2010**, *17*, 2990–3006.

(19) Nie, Q.; Du, X. G.; Geng, M. Y. Small molecule inhibitors of amyloid beta peptide aggregation as a potential therapeutic strategy for Alzheimer's disease. *Acta Pharmacol. Sin.* **2011**, *32*, 545–551.

(20) Pey, A. L.; Ying, M.; Cremades, N.; Velazquez-Campoy, A.; Scherer, T.; Thony, B.; Sancho, J.; Martinez, A. Identification of pharmacological chaperones as potential therapeutic agents to treat phenylketonuria. *J. Clin. Invest.* **2008**, *118*, 2858–2867.

(21) Cremades, N.; Velazquez-Campoy, A.; Martinez-Julvez, M.; Neira, J. L.; Perez-Dorado, I.; Hermoso, J.; Jimenez, P.; Lanás, A.; Hoffman, P. S.; Sancho, J. Discovery of specific flavodoxin inhibitors as potential therapeutic agents against *Helicobacter pylori* infection. *ACS Chem. Biol.* **2009**, *4*, 928–938.

(22) Benkemoun, L.; Sabate, R.; Malato, L.; Dos Reis, S.; Dalstra, H.; Saupe, S. J.; Maddelein, M. L. Methods for the in vivo and in vitro analysis of [Het-s] prion infectivity. *Methods* **2006**, *39*, 61–67.

(23) Morell, M.; de Groot, N. S.; Vendrell, J.; Aviles, F. X.; Ventura, S. Linking amyloid protein aggregation and yeast survival. *Mol. Biosyst.* **2011**, *7*, 1121–1128.

(24) LeVine, H., III. Thioflavine T interaction with synthetic Alzheimer's disease beta-amyloid peptides: detection of amyloid aggregation in solution. *Protein Sci.* **1993**, *2*, 404–410.

(25) Lipinski, C. A.; Lombardo, F.; Dominy, B. W.; Feeney, P. J. Experimental and computational approaches to estimate solubility and permeability in drug discovery and development settings. *Adv. Drug Delivery Rev.* **2001**, *46*, 3–26.

(26) Coustou-Linares, V.; Maddelein, M. L.; Begueret, J.; Saupe, S. J. In vivo aggregation of the HET-s prion protein of the fungus *Podospora anserina*. *Mol. Microbiol.* **2001**, *42*, 1325–1335.

(27) Ritter, C.; Maddelein, M. L.; Siemer, A. B.; Luhrs, T.; Ernst, M.; Meier, B. H.; Saupe, S. J.; Riek, R. Correlation of structural elements and infectivity of the HET-s prion. *Nature* **2005**, *435*, 844–848.

(28) Greenwald, J.; Buhtz, C.; Ritter, C.; Kwiatkowski, W.; Choe, S.; Maddelein, M. L.; Ness, F.; Cescau, S.; Soragni, A.; Leitz, D.; Saupe, S. J.; Riek, R. The mechanism of prion inhibition by HET-S. *Mol. Cell* **2010**, *38*, 889–899.

(29) Carroll, A.; Sweigard, J.; Valent, B. Improved vectors for selecting resistance to hygromycin. *Fungal Genet. Newsl.* **1994**, *41*, 42.

(30) Link, C. D. Expression of human beta-amyloid peptide in transgenic *Caenorhabditis elegans*. *Proc. Natl. Acad. Sci. U.S.A.* **1995**, *92*, 9368–9372.

(31) Griffiths, A. J. Fungal senescence. *Annu. Rev. Genet.* **1992**, *26*, 351–372.

(32) Halfmann, R.; Lindquist, S. Screening for amyloid aggregation by Semi-Denaturing Detergent-Agarose Gel Electrophoresis. *J. Visualized Exp.* **2008**, doi 10.3791/838.